



HAL
open science

The elastocapillary ridge as a non-integer disclination

Robin Masurel, Matthieu Roché, Laurent Limat, Ioan Ionescu, Julien Dervaux

► **To cite this version:**

Robin Masurel, Matthieu Roché, Laurent Limat, Ioan Ionescu, Julien Dervaux. The elastocapillary ridge as a non-integer disclination. *Physical Review Letters*, 2019, 122 (24), pp.248004. hal-01818872v2

HAL Id: hal-01818872

<https://hal.science/hal-01818872v2>

Submitted on 4 Feb 2019

HAL is a multi-disciplinary open access archive for the deposit and dissemination of scientific research documents, whether they are published or not. The documents may come from teaching and research institutions in France or abroad, or from public or private research centers.

L'archive ouverte pluridisciplinaire **HAL**, est destinée au dépôt et à la diffusion de documents scientifiques de niveau recherche, publiés ou non, émanant des établissements d'enseignement et de recherche français ou étrangers, des laboratoires publics ou privés.

The elastocapillary ridge as a non-integer disclination

Robin Masurel,¹ Matthieu Roché,¹ Laurent Limat,¹ Ioan Ionescu,² and Julien Dervaux^{1,*}

¹Laboratoire Matière et Systèmes Complexes, Université Paris Diderot, CNRS UMR 7057, Sorbonne Paris Cité, 10 Rue A. Domon et L. Duquet, F-75013 Paris, France

²Laboratoire des Sciences des Procédés et des Matériaux, Université Paris 13, CNRS UPR 3407, Sorbonne Paris Cité, 99 Avenue J.-B. Clément, F-93430 Villetaneuse, France

(Dated: February 4, 2019)

Understanding interfacial properties of solids with their environment is a crucial problem in fundamental science and applications. Elastomers have challenged the scientific community in this respect, and a satisfying description is still missing. Here, we argue that the interfacial properties of elastomers, such as their wettability, can be understood only with a non-linear elastic model with the assumption of strain-independent surface energy. We show that our model captures accurately available data on elastomer wettability and discuss its implications.

In his founding paper on the thermodynamics of interfaces [1], Gibbs defines the surface energy γ of a material as the work required to create a unit area by bringing new molecules in contact with the atmosphere, cutting bulk interatomic bonds and maintaining a constant intermolecular distance. Also, he highlights the conceptual difference between γ and the surface tension Υ of the interface, defined as the work required to create a unit surface by stretching the material at constant number of molecules in the interface (see ref. [2] for a concise summary). The difference stems from the ability of molecules to rearrange under stretch, *e.g.* $\gamma = \Upsilon$ in liquids [3, 4]. Molecules in an elastic solid cannot move. Stretching a solid alters the intermolecular distance so that $\gamma \neq \Upsilon$ in general. These two quantities are related through the Shuttleworth-Herring equation [4]: $\Upsilon(\hat{\lambda}) = \gamma(\hat{\lambda}) + \partial\gamma/\partial\hat{\lambda}$ where $\hat{\lambda}$ is a two-dimensional strain tensor in the plane of the interface. Reliable measurements of $\Upsilon(\hat{\lambda})$ and $\gamma(\hat{\lambda})$ exist for various metals [3, 5–8].

The surface energy of a material can be adjusted with a chemical treatment, such as monolayer deposition or coating. In this perspective, elastomers, *i.e.* crosslinked polymer melts, have attracted interest in recent years [9–17]. However, the definition of γ for these amorphous layers poses challenges that have yet to be met. In particular, studies of the dependence of $\gamma(\lambda)$ in the context of elastomer wetting (or elastowetting) have led to contradictory conclusions [10, 14, 15, 18].

Here, we show that a finite-deformation model of elastomers under the assumption of a strain-independent surface energy provides an excellent description of the wetting and adhesion of elastomers. First we motivate the need for a non-linear mechanical model and we justify the assumption of strain-independent surface energy. Then, we present our model. A central result of our rationale is that the deformation of the solid below the contact line has the features of a disclination. This result opens the possibility of studying wetting ridges as defects induced by the presence of contact lines. We demonstrate that our model is in very good agreement with available experimental data. Finally, we discuss the validity of other assumptions used in linear models of elastowetting.

Up to now, scientists have modelled wetting and adhesion on elastomers with linear elasticity, *i.e.* infinitesimal defor-

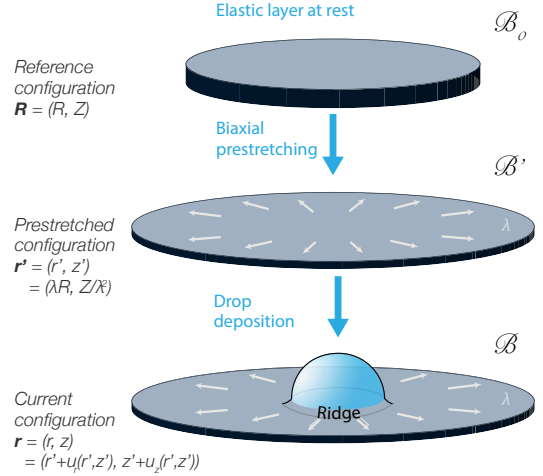


FIG. 1. Schematic representation of the problem. A flat layer with initial thickness H and infinite lateral dimensions (state \mathcal{B}_0) is first biaxially stretched (state \mathcal{B}'). A drop is then deposited on this stretched surface and further deforms the elastic layer (state \mathcal{B}).

mations are assumed. This hypothesis holds only for $\lambda \simeq 1$ and $\gamma_\ell/2\gamma_s \ll 1$, with γ_ℓ the liquid surface tension and γ_s the elastomer surface tension. However, experiments never meet these requirements, as $0.5 \lesssim \gamma_\ell/2\gamma_s \lesssim 0.9$ and $1 \lesssim \lambda \lesssim 2$. Besides, crosslinking is not a liquid-solid phase transition and thus elastomers respond like solids at the macroscopic scale but they remain liquid at the microscopic scale [19, 20]. Rubber elasticity arises from the entropic cost of stretching polymer chains [21, 22], a process that still allows the position of the monomers to fluctuate. As a consequence, monomers in the bulk can move to the surface of the stretched sample: the cost of creating a unit elastomer surface should be strain-independent. This view is supported by experiments [15, 23] and recent numerical simulations [14].

Following these remarks, we consider a flat incompressible layer, made of a homogeneous isotropic incompressible Neo-Hookean material, with initial thickness H and infinite lateral dimensions described in cylindrical coordinates by the region

$0 \leq R < \infty$ and $0 \leq Z \leq H$ (Fig. 1) as the reference configuration \mathcal{B}_0 of our description. This layer is biaxially stretched such that a material point with position $\mathbf{R} = (R, Z)$ is mapped to a position $\mathbf{r}' = (r', z') = (\lambda R, Z/\lambda^2)$ in configuration \mathcal{B}' . The thickness of the prestretched layer is thus $h = H/\lambda^2$. Deformation is locally described by the deformation tensor $\mathbf{F}' = \partial \mathbf{r}' / \partial \mathbf{R}$. Finally, a drop deposited at the free surface of the prestretched layer induces an additional deformation, superposed on the previous finite deformation, leading to the formation of an elastocapillary ridge. Thus, another deformation field maps a point with coordinates \mathbf{r}' in configuration \mathcal{B}' to a position $\mathbf{r} = \mathbf{r}' + \mathbf{u}(\mathbf{r}') = (r' + u_r(r', z'), z' + u_z(r', z'))$ in the current configuration \mathcal{B} . Note that deformation from \mathcal{B}' to \mathcal{B} is expressed in the prestretched coordinates (r', z') . The deformation tensor $\mathbf{F} = \partial \mathbf{r} / \partial \mathbf{R}$ is a local description of the overall deformation process. The strain energy density of the layer is $\mathcal{W}_e = \frac{\mu}{2} (\text{Tr} \mathbf{F}^T \mathbf{F} - 3)$. Following the ideas exposed in the introduction, we assume that the system also has a strain-independent surface energy density $\mathcal{W}_s = \gamma_s$ in the current configuration \mathcal{B} . Furthermore, we account for the incompressibility constraint $\det \mathbf{F} = 1$ by introducing a Lagrange multiplier P , interpreted as a pressure. The total energy functional $\mathcal{E}[\mathbf{r}, \boldsymbol{\rho}, P]$ of the system then reads:

$$\mathcal{E}[\mathbf{r}, \boldsymbol{\rho}, P] = \frac{\mu}{2} \int_{\mathcal{B}_0} (\text{Tr}(\mathbf{F}^T \mathbf{F}) - 3) dV + \gamma_s \int_{\partial \mathcal{B}} da - \int_{\mathcal{B}_0} P (\det \mathbf{F} - 1) dV - \int_{\partial \mathcal{B}'} \mathbf{f} \cdot \mathbf{u} da' \quad (1)$$

where $\boldsymbol{\rho} = \{\rho, d\}$ is the position of the contact line, dV is an infinitesimal volume in the reference configuration while da (resp. da') is an infinitesimal element of area in the current (resp. prestretched) configuration \mathcal{B} (resp. \mathcal{B}'). Vector \mathbf{f} describes the force distribution applied at the free surface of the elastic layer by the drop. For a hemispherical drop with radius ρ , surface energy γ_ℓ and macroscopic contact angle α , \mathbf{f} has two contributions: a localized traction $\mathbf{f}^T = \gamma_\ell \delta(r' - \rho) (\sin \alpha \mathbf{e}_z - \cos \alpha \mathbf{e}_r)$ at the triple line and a distributed compression $\mathbf{f}^c = -\gamma_\ell \sin \alpha / \rho \Pi(\rho - r') \mathbf{e}_z$ below the drop due to Laplace pressure, with Π the Heaviside function.

We obtain the equilibrium equations describing the system from the principle of stationary potential energy: energy variations $\delta \mathcal{E}[\mathbf{r}, \boldsymbol{\rho}, P]$ due to small variations in the independent fields must be zero. We close the system by providing boundary conditions. Inspired by experimental setups, we assume that the lower surface of the elastic layer is bonded to an infinitely rigid surface, $u_r(r', 0) = u_z(r', 0) = 0$. From Eq. 1, we find the first Piola-Kirchoff tensor $\mathbf{P} = \mu \mathbf{F} - P \mathbf{F}^{-1}$. Recalling that $\mathbf{F}' = \partial \mathbf{r}' / \partial \mathbf{R}$, the equilibrium equation can be written as $\text{div}(\mathbf{P} \mathbf{F}') = \mathbf{0}$ where the div operator is evaluated in the prestretched configuration \mathcal{B}' . Everywhere at the free boundary $z' = h$ except at the triple line, Nanson's formula gives $\mathbf{P} \mathbf{F}' \cdot \mathbf{n}' = \mathbf{f}^c + \gamma_s \mathbf{n} \cdot (\nabla \mathbf{n})$ where $\mathbf{n}' = (0, 1)$ is the outward unit vector normal to the free surface in \mathcal{B}' and \mathbf{n} is the outward unit normal vector in \mathcal{B} .

From the variation of the energy with respect to $\boldsymbol{\rho}$, we ob-

tain the force balance at the triple line [24–26]:

$$-\gamma_\ell \cos \alpha = \gamma_s \{ \cos \theta^- - \cos \theta^+ \} + \mathbf{e}_r \cdot \mathbf{f}^E \text{ along } \mathbf{e}_r \quad (2)$$

$$\gamma_\ell \sin \alpha = \gamma_s \{ \sin \theta^- + \sin \theta^+ \} + \mathbf{e}_z \cdot \mathbf{f}^E \text{ along } \mathbf{e}_z \quad (3)$$

where $\theta^- = |\partial u_z / \partial r(\rho^-, 0)|$ and $\theta^+ = |\partial u_z / \partial r(\rho^+, 0)|$ are the (positive) slopes of the solid surface on each side of the triple line. The jump in the first derivative of the displacement field ($\partial u_z / \partial r(\rho^-, 0) \neq \partial u_z / \partial r(\rho^+, 0)$) induces a logarithmic divergence of the stress. Thus the contact line is a singular structure known as a disclination [27] in Eshelbian mechanics whose strength, given by $1/2 - \theta/2\pi$, can take any value between $-1/2$ and $1/2$ as there is no underlying lattice structure, in contrast with disclinations in crystals. The last terms in Eqs. 2-3 involve the Eshelby force \mathbf{f}^E acting on an elastic singularity [28, 29]:

$$\mathbf{f}^E = \lim_{\varepsilon \rightarrow 0} \int_{\Gamma'_\varepsilon} (\mathcal{W}_e \mathbf{I} - \mathbf{F}^T \mathbf{P}) \boldsymbol{\nu}' d\ell' \quad (4)$$

where Γ'_ε is a contour of radius ε enclosing the defect in \mathcal{B}' and $\boldsymbol{\nu}'$ is the outward unit normal vector to the contour; \mathbf{f}^E has the dimensions of a force per unit length and it is the J-integral in fracture mechanics [30]. Equations (2)-(3) are new generalized laws for contact angles of liquid drops on soft materials.

Equations 2-3 present interesting limiting cases. Fluids are described using the current (deformed) configuration as reference, in which case $\mathbf{F} = \mathbf{I}$. The first Piola-Kirchoff stress tensor then reduces to the Cauchy stress tensor which, at rest, is just a pressure, $\mathbf{P} = -p \mathbf{I}$. The contour integral (4) vanishes [31], leading to the Neumann construction that rules the force balance at a triple line between fluids. In contrast, shear stresses between fluids in relative motion induce configurational forces at the triple line [31]. On a soft substrate without hysteresis, \mathbf{f}^E vanishes in the framework of linear elasticity, *i.e.* when $\gamma_\ell / 2\gamma_s \rightarrow 0$, and the liquid surface tension is balanced by the surface energy of the solid. When the substrate is infinitely rigid, θ^- and θ^+ vanish and Eq. 2 reduces to a generalized Young equation with line tension [32]. Equation 3 indicates that the vertical surface traction is balanced by elasticity for hard materials [33].

We solve Eqs 1-4 using a numerical method that we developed earlier [34]. For all simulations, $H = 80 \mu\text{m}$, similar to typical values encountered in experiments, and $\alpha = \pi/2$. The volume of the droplet is $5 \mu\text{L}$ and its radius $\rho \sim 1.33 \text{ mm}$, to minimize the influence of the finite size of the drop. In the supplementary materials, we derive an analytical solution to the elastowetting problem in the framework of incremental elasticity, where the amplitude of the displacement field \mathbf{u} superimposed to prestretch is of the order of a small parameter ε . Figure 2B shows that the incremental theory provides an excellent approximation to the numerical simulations of the nonlinear problem for the shape of the ridge for $\lambda = 1$, at both large ($r \gtrsim \ell_s = \gamma_s / (2\mu)$) and small ($r \lesssim \ell_s$) scale. When $\lambda = 1.5$, we observe poor agreement between the incremental theory and the numerical simulations (Fig. 2C): the latter

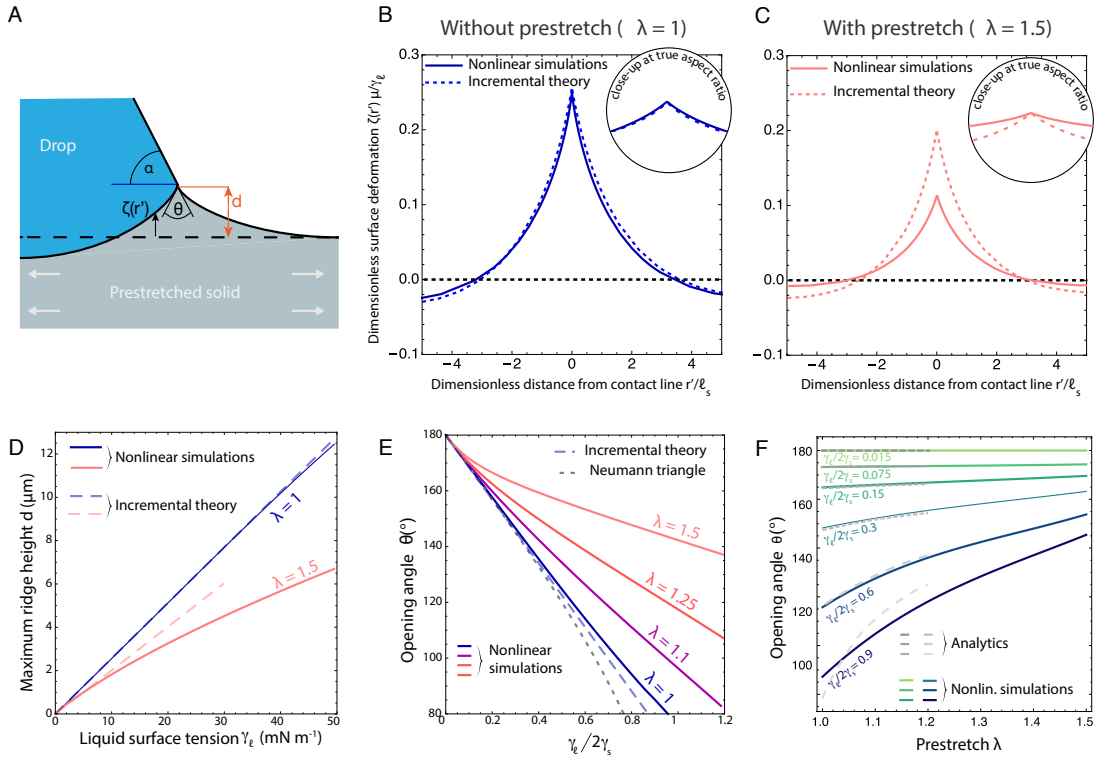


FIG. 2. Comparison between the linear and non-linear elastic models. A: schematic of the region around the elastocapillary ridge with maximum height d , height profile $\zeta(r')$ and opening angle at the tip θ . Shape of the ridge with (B) and without (C) prestretch, for $\gamma_\ell/2\gamma_s = 0.8$. Insets in B and C: zoomed-in shape of the ridge (over a total width ℓ_s) at true aspect ratio (*i. e.* same normalization for height and width by ℓ_s). The linear model and the numerical simulations have been shifted so that tips coincide for better comparison. D: Maximum ridge height d as a function of the liquid surface tension γ_ℓ for a solid surface tension $\gamma_s = 30 \text{ mN m}^{-1}$. E: opening angle θ as a function of the ratio $\gamma_\ell/2\gamma_s$ for $1 \leq \lambda \leq 1.5$. F: opening angle θ as a function of prestretch λ for $0.015 \leq \gamma_\ell/2\gamma_s \leq 0.9$. Light dashed lines: Eq 7.

predicts a ridge height smaller than expected from the incremental theory and the opening angle θ of the ridge is larger. Figure 2D indicates that, in presence of prestretch, numerical simulations coincide with the incremental solution only at small values of the ratio $\gamma_\ell/2\gamma_s$, for $\gamma_s = 30 \text{ mN m}^{-1}$. The agreement between the two models is very good For $\lambda = 1$.

A focus on the dependence of θ on control parameters (λ , γ_ℓ/γ_s) allows us to discuss the nature of the force balance at the contact line. We compare the results of our simulations to the Neumann construction, $\theta = \pi - 2\arcsin(\gamma_\ell/2\gamma_s)$, and its linearized version for small angles, $\theta = \pi - \gamma_\ell/\gamma_s$. The opening angle θ decreases with increasing value of the ratio $\gamma_\ell/2\gamma_s$ for all models (Fig. 2E). For $\lambda = 1$ and for values of $\gamma_\ell/2\gamma_s$ up to ~ 0.9 , the linearized Neumann construction approximates the nonlinear elastowetting problem well, with an error smaller than 5%. For $\gamma_\ell/2\gamma_s \gtrsim 0.9$, θ is larger than predicted by the linear theory, with the difference increasing with $\gamma_\ell/2\gamma_s$. At the same time, the full Neumann construction fails at following the non-linear prediction. For $\gamma_\ell/2\gamma_s \sim 0.9$, typical of silicone/water experiments, the non-linear prediction of θ is 30° larger than the prediction based on the Neumann construction. This difference is much larger than the precision of typical experimental measurements. The non-linear model

indicates that θ increases monotonously with λ (Fig. 2E-F). This results contradicts the predictions of linear theories, in which θ is independent of λ . Thus, this dependence is a pure nonlinear effect.

Analytical considerations can help clarify the mechanics behind the dependence of the opening angle θ on deformation λ (Fig. 2F). The stress field around the elastocapillary ridge is equivalent to that around a wedge disclination. In linear elasticity [35–37], the Eshelby force (4) for a disclination line in an external stress field is: $\mathbf{f}^E \approx -2\mathbf{e}_\theta \times (2\pi\mathbf{S}\mathbf{M} \cdot \mathbf{e}_\theta)$. Here $M_{jm} = T_{ji}\epsilon_{imn}u_n(R)$ is the torque on the defect, T_{ji} is the Cauchy stress, ϵ_{imn} is the Levi-Civita tensor. Einstein summation convention applies. The factor of 2 results from the presence of the free surface that acts as a mirror disclination of opposite strength $-S$. At leading order, the vertical component of the Eshelby force acting on the ridge is:

$$f_z^E \approx 4\pi ST_{rr}^{(0)} \zeta(R) = 2\mu(\pi - \theta)(\lambda^2 - \frac{1}{\lambda^4})\zeta(R) \quad (5)$$

Equation 5 is equivalent to the Peach-Koehler force acting on a dislocation [38]. Indeed, the vertical component of the Peach-Koehler force on a surface dislocation reads $-2[T_{rz}u_z]$ where the bracket operator $[f]$ denotes the jump of f across

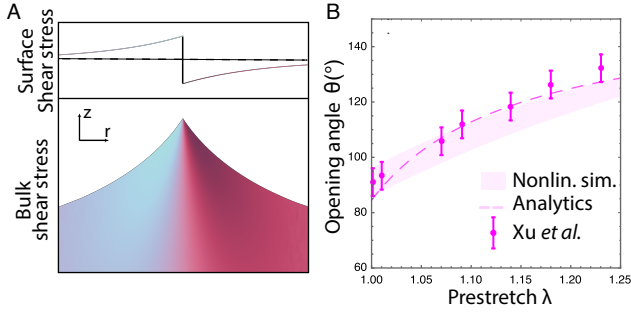


FIG. 3. A: Shear stress distribution in the ridge below the triple line obtained from the numerical simulations ($\lambda = 1.2$, $\gamma_\ell/\gamma_s = 0.8$; other parameters identical to those of Fig. 2). Size of the box: $2\ell_s \times 2\ell_s$. Upper panel: shear stress jump at the free surface across the contact line. B: comparison between Xu *et al.*'s data [10], our numerical simulations and Eq. 7 for $\theta(\lambda)$.

the defect. For a dislocation, the stress field is continuous while the jump of the displacement u_z is non-zero (and defined as the Burger vector). In our case, the boundary condition at the free surface imposes that $T_{rz} = T_{rr}^{(0)} \partial \zeta / \partial r'$. Displacement u_z is thus continuous while the shear stress is discontinuous (Fig. 3A). We recover Eq. 5 if we inject T_{rz} in the Peach-Koehler expression or by the direct integration of (4) (see SI). The force f_z^E is independent of the elastic modulus because the height of the ridge is inversely proportional to the substrate shear modulus, $\zeta(\rho) = a(\rho, H) \gamma_\ell \sin \alpha / (\mu g_\infty(\lambda))$ (See SI for a definition of g_∞). Here $a(\rho, H)$ is a geometric parameter that is weakly dependent on the thickness H and the droplet size ρ , provided that both are larger than the elastocapillary length ℓ_s , and whose value is $a(\rho, H) \sim 0.25$. Thus we have the approximation $f_z^E \approx \gamma_\ell \sin \alpha / (2g_\infty(\lambda)) (\lambda^2 - 1/\lambda^4) (\pi - \theta)$. The Eshelby force f_z^E is equivalent to an effective surface energy of magnitude $\gamma_\ell \sin \alpha / (2g_\infty(\lambda)) (\lambda^2 - 1/\lambda^4)$ whose origin is purely topological. As a consequence, we define an "apparent surface tension" Υ at the ridge tip:

$$\Upsilon \approx \gamma_s \left\{ 1 + \frac{\gamma_\ell \sin \alpha}{\gamma_s} \frac{\lambda^9 + \lambda^6 - \lambda^3 - 1}{\lambda^9 + \lambda^6 + 3\lambda^3 - 1} \right\} \quad (6)$$

which reduces to $\Upsilon \approx \gamma_s \{1 + 3\gamma_\ell \gamma_s^{-1} \sin \alpha (\lambda - 1)\}$ at small λ . Eq. 6 leads to the following approximation for the opening angle:

$$\theta \approx \pi - \frac{\gamma_\ell}{\Upsilon} \quad (7)$$

Eqs. 6-7 result from a crude approximation of the Eshelby force as we have neglected the force of the disclination on itself as well as the force induced by Laplace pressure on the defect. These contributions of higher order than the leading term (Eq. 5) can become significant when $\gamma_\ell/2\gamma_s = \mathcal{O}(1)$, even in the case $\lambda = 1$ (Fig. 2E). Nonetheless, Eq. 7 provides a reasonable approximation for θ (Fig. 2F). The existence of an elastic restoring force proportional to ζ and μ was reported in recent molecular dynamics simulations [13].

Now we compare our theoretical predictions to available experimental data. Xu *et al.* measure an opening angle $\theta = 91.2^\circ$ in their glycerol-silicone system, with $\gamma_{Gly} = 41 \pm 1 \text{ mN m}^{-1}$ [10]. The surface energy of PDMS deduced from the Neumann construction is $\gamma_s = 29 \text{ mN m}^{-1}$. Our nonlinear model yields $\gamma_s = 24 \text{ mN m}^{-1}$, in better agreement with the surface energy of liquid PDMS, $\gamma_{PDMS} = 21 \pm 1 \text{ mN m}^{-1}$. Fig. 3B shows that our numerical simulations capture well Xu *et al.*'s data for $\theta(\lambda)$. In addition, we obtain excellent agreement between experiments and Eq. 7 (Fig. 2F and 3B).

Within the experimental error bars, we conclude that Xu *et al.*'s observations result from the nonlinear elastic force \mathbf{f}^E acting on the elastocapillary ridge. From the assumptions of our model based on mechanical and molecular considerations and the good agreement between experiments and theory, we conclude that soft elastomers have a strain-independent surface energy, *i.e.* the Shuttleworth effect does not exist for elastomers in this range of deformations, in agreement with recent experimental and numerical results [14, 15]. Moreover, results in Fig. 2 indicate that the Neumann construction does not hold for values of $\gamma_\ell/2\gamma_s$ typical of experiments, whatever the deformation of the substrate. We note that the apparent surface tension defined in Eq. 6 appears in the force balance at the tip of the ridge as a consequence of the corner singularity; Υ cannot be used as a pseudo-Shuttleworth effect that would apply everywhere at the surface of the elastomer. Finally, remarkable predictions arise from Eq. 6. First, Υ decreases under compression and vanishes at $\lambda_0 \approx 0.82$. Second, the Peach-Koehler force exceeds the restoring force of the solid surface for $\lambda_c \leq \lambda \leq \lambda_0$, where $\lambda_c \approx 0.666$ is the critical stretch of the Biot instability [39]. In this range of λ , Υ is negative. Current experimental work in our group investigates this region of the parameter space.

To conclude, we have unraveled a general balance of forces (Eqs. 2-3) at contact lines on soft materials based on nonlinear elasticity under the assumption of strain-independent surface energy. We predict quantitatively the strain dependence of the angle at the apex of the elastocapillary ridge below a three-phase contact line that we show to result from mechanical non-linearities. We bring evidence of the invalidity of the Neumann construction in elastocapillarity. A key result is that the ridge is equivalent to a non-integer disclination. We expect our work to have implications in the control of droplet interactions on soft surfaces and the study of elastowetting dynamics [11, 12, 40] as the disclination force is an additional dissipation source. Finally, our theoretical framework should help understand the formation of elastic singularities such as cusps in the Biot instability [41-44].

We thank Cyprien Gay and Suzie Protière for discussions. ANR (Agence Nationale de la Recherche) and CGI (Commissariat à l'Investissement d'Avenir) are gratefully acknowledged for their financial support through the GELWET project (ANR-17-CE30-0016), the Labex SEAM (Science and Engineering for Advanced Materials and devices - ANR 11 LABX 086, ANR 11 IDEX 05 02) and through the funding of the POLYWET and MMEMI projects.

* julien.dervaux@univ-paris-diderot.fr

- [1] J. W. Gibbs, in *Sci. Pap. J. W. Gibbs* (Longmans, Green and Co., London, New York and Bombay, 1906), vol. 1, pp. 55–353.
- [2] A. I. Rusanov, *Surf. Sci. Rep.* **23**, 173 (1996).
- [3] P. Müller and A. Saúl, *Surf. Sci. Rep.* **54**, 157 (2004).
- [4] A. I. Rusanov, *Surf. Sci. Rep.* **58**, 111 (2005).
- [5] R. C. Cammarata, *Prog. Surf. Sci.* **46**, 1 (1994).
- [6] M. C. Payne, N. Roberts, R. J. Needs, M. Needels, and J. D. Joannopoulos, *Surf. Sci.* **211-212**, 1 (1989).
- [7] V. Fiorentini, M. Methfessel, and M. Scheffler, *Phys. Rev. Lett.* **71**, 1051 (1993).
- [8] H. Ibach, *Surf. Sci. Rep.* **29**, 195 (1997).
- [9] R. W. Style, A. Jagota, C. Y. Hui, and E. R. Dufresne, *Annu. Rev. Condens. Matter Phys.* **8**, 99 (2017).
- [10] Q. Xu, K. E. Jensen, R. Boltyanskiy, R. Sarfati, R. W. Style, and E. R. Dufresne, *Nat. Commun.* **8**, 555 (2017).
- [11] M. Zhao, F. Lequeux, T. Narita, M. Roché, L. Limat, and J. Dervaux, *Soft Matter* **14** (2017).
- [12] M. Zhao, J. Dervaux, T. Narita, F. Lequeux, L. Limat, and M. Roché, *Proc. Nat. Acad. Sci. U.S.A.* **115**, 1748 (2018).
- [13] H. Liang, Z. Cao, Z. Wang, and A. V. Dobrynin, *Langmuir* **34**, 7497 (2018).
- [14] H. Liang, Z. Cao, Z. Wang, and A. V. Dobrynin, *ACS Macro Lett.* **7**, 116 (2018).
- [15] R. D. Schulman, M. Trejo, T. Salez, E. Raphaël, and K. Dalnoki-Veress, *Nat. Commun.* **9**, 982 (2018).
- [16] Q. Xu, R. W. Style, and E. R. Dufresne, *Soft Matter* **14**, 916 (2018).
- [17] J. H. Snoeijer, E. Rolley, and B. Andreotti, *Phys. Rev. Lett.* **121**, 68003 (2018).
- [18] R. D. Schulman and K. Dalnoki-Veress, *Phys. Rev. Lett.* **115**, 206101 (2015).
- [19] P. J. Flory, *Principles of Polymer Chemistry* (Cornell University Press, New York, 1953).
- [20] M. Rubinstein and S. Panyukov, *Macromolecules* **30**, 8036 (1997).
- [21] L. R. G. Treloar, *The physics of rubber elasticity* (Oxford University Press, 1975), 3rd ed.
- [22] A. Y. Grosberg and A. R. Khokhlov, *Giant Molecules, Here, There and Everywhere* (World Scientific Publishing, Singapore, 2011), 2nd ed.
- [23] C. Gay, *Int. J. Adhes. Adhes.* **20**, 387 (2000).
- [24] I. M. Gelfand and S. V. Fomin, *Calculus of variations* (Dover Publications, 2000).
- [25] P. Podio-Guidugli, *Interfaces Free Boundaries* **3**, 223 (2001).
- [26] A. Gupta and X. Markenscoff, *C. R. Mec.* **336**, 126 (2008).
- [27] P.-G. de Gennes and J. Prost, *The physics of Liquid crystals* (Oxford Science Publications, Oxford, 1995), 2nd ed.
- [28] J. D. Eshelby, *Philos. Trans. R. Soc. London. Ser. A, Math. Phys. Sci.* **244**, 87 LP (1951).
- [29] J. D. Eshelby, *J. Elast.* **5**, 321 (1975).
- [30] J. R. Rice, *Conserved integrals and energetic forces* (Cambridge University Press, Cambridge, 1985).
- [31] M. E. Gurtin, *Configurational forces as basic concepts of continuum physics* (Springer, Berlin, 2000).
- [32] A. I. Rusanov, *Colloid J. USSR* **39**, 618 (1977).
- [33] J. Dervaux and L. Limat, *Proc. R. Soc. A* **471**, 20140813 (2015).
- [34] R. de Pascalis, J. Dervaux, I. Ionescu, and L. Limat, *Eur. J. Mech. - A/Solids* **71**, 151 (2018).
- [35] T. Mura, *Fundam. Asp. Dislocation Theory* **2** (1970).
- [36] V. Vitek and M. Kléman, *J. Phys.* **36**, 59 (1975).
- [37] J. D. Eshelby, in *Mech. Solids*, edited by H. G. Hopkins and M. J. B. T. Sewell (Pergamon, Oxford, 1982), pp. 185–225.
- [38] M. Peach and J. S. Koehler, *Phys. Rev.* **80**, 436 (1950).
- [39] M. A. Biot, *Appl. Sci. Res. Sect. A* **12**, 168 (1963).
- [40] S. Karpitschka, S. Das, M. van Gorcum, H. Perrin, B. Andreotti, and J. H. Snoeijer, *Nat. Commun.* **6**, 7891 (2015).
- [41] J. Dervaux, Y. Couder, M.-A. Guedeau-Boudeville, and M. Ben Amar, *Phys. Rev. Lett.* **107**, 018103 (2011).
- [42] J. Dervaux and M. Ben Amar, *J. Mech. Phys. Solids* **59**, 538 (2011).
- [43] E. Hohlfeld and L. Mahadevan, *Phys. Rev. Lett.* **106**, 105702 (2011).
- [44] S. Karpitschka, J. Eggers, A. Pandey, and J. H. Snoeijer, *Phys. Rev. Lett.* **119**, 198001 (2017).